

Electrocatalytic Reduction of Dioxygen on 9,10-Anthraquinones-Incorporated Clay-Modified Glassy Carbon Electrodes

Paramasivam Manisankar* **and Anandhan Gomathi**[1]

Department of Chemistry, Periyar University, Salem 636 011, India

[1]Department of Chemistry, A.K.G.S Arts College, Srivaikuntam 628 619, India

Received December 14, 2004; E-mail: pms11@rediffmail.com

The preparation and electrochemical characterization of 9,10-anthraquinones adsorbed clay-modified and anthraquinones–clay composite-modified glassy carbon electrodes (GCEs) were investigated. The influence of the pH on the electrochemical behavior and stability of the clay-modified electrodes (CMEs) were studied by cyclic voltammetry in acidic and neutral aqueous media. For the dioxygen reduction, anthraquinones adsorbed clay-modified electrodes possess good electrocatalytic abilities with overpotential ranging from 174 to 452 mV, lower than the bare GCE in the pH range 4.0–7.0; also, anthraquinones–clay composite-modified electrodes exhibited potent catalytic activities with an overpotential of about 128–421 mV lower than at a bare GCE at pH 7.0–8.0. The diffusion coefficients of mediators in clay films were evaluated by chronoamperometric techniques. Chronocoulometric studies showed the involvement of two electrons in the reduction of anthraquinones and four electrons in dioxygen reduction at the optimum pH. In addition, hydrodynamic voltammetric studies were performed to determine the mass-specific activity of the anthraquinones used, the heterogeneous rate constants for the reduction of O_2 at the surface of modified electrodes and the apparent diffusion coefficient of O_2 in aqueous O_2-saturated buffer solutions.

Dioxygen reduction in energy conversion and storage and in the development of biosensors has led to an effort to find new catalysts and modified electrodes in recent years.[1–7] A small amount of catalyst is needed for reduction when immobilized modifiers and mediators are employed.[8] Modification of the electrode surface by thin films of clay colloids has been the subject of interest in recent years, because of their imperfect stacks of clay layers.[9,10]

The electrochemical behavior of montmorillonite clay-modified electrodes (CMEs) strongly depends on the incorporated adsorbed electroactive species.[11] A wide variety of compounds, such as copper,[12] manganese oxide,[13] ruthenium–iron cluster,[14] titanium silicates,[15] Au nanoparticle,[16] metal phthalocyanine,[17] cobalt complexes,[3] metal macrocyclic complexes,[1,18] pyrimidine bases,[19] naphthoquinone,[20,21] and anthraquinone[22–25] derivatives, have been proposed as electrocatalysts for the reduction of dioxygen to water or H_2O_2. Dioxygen reduction to H_2O_2 is a two-electron reaction and four-electron reduction leads to the formation of water. The photoelectrochemistry of thionine dye-incorporated clay-modified electrodes was examined by Kamat, who used them in the conversion of light energy into electricity.[26] Catalysis of electroreduction of H_2O_2 was investigated by Oyama et al.[27] on Ru$(NH_3)_6^{3+}$-incorporated montmorillonite clay-modified graphite electrodes and by Zen et al.[28] on methyl viologen-incorporated nontronite clay-coated glassy carbon electrodes. Electrocatalytic dioxygen reduction was also reported by Oyama[29] on a poly(viologen)–poly(sulfonate) complexes modified graphite electrode and by Hu[30] on a sodium montmorillonite–methyl viologen carbon paste chemically modified electrode. Fukuzumi et al. reported on the dehydrogenation of 10-methyl-9,10-dihydroacridine by oxygen, accompanied by the two-electron and four-electron reduction of O_2 to produce H_2O_2 and H_2O which were effectively catalyzed by monomeric cobalt porphyrins and cofacial dicobalt porphyrins in the presence of perchloric acid in acetonitrile and benzonitrile, respectively.[31] However, the use of anthraquinone-incorporated sodium montmorillonite clay-modified glassy carbon electrodes in dioxygen reduction has not been explored so far.

In the present work, the electrochemical behavior of anthraquinone, its amino derivatives and dyes incorporated clay-modified glassy carbon electrodes, the efficiency and stability of these modified electrodes in the electrocatalysis of dioxygen reduction to water were examined by cyclic voltammetry, chronoamperometry, chronocoulometry, and rotating-disk electrode voltammetry along with the determination of diffusional and kinetic parameters.

Experimental

Reagents. 9,10-Anthraquinone (AQNE), 1-amino anthraquinone (1-AMAQ), 2-amino anthraquinone (2-AMAQ), and 1,4-diamino anthraquinone (DIAMAQ) were purchased from Lancaster. Disperse blue 3 (DB3), Disperse blue 26 (DB26), and Disperse red 11 (DR11) (Scheme 1) were received as samples from ATUL India Ltd. and purified before use. HPLC-grade acetonitrile (SRL) was used as received. 0.001 M solutions of anthraquinone derivatives and dyes were prepared in acetonitrile. The aqueous solutions used at different pH values were 0.1 M H_2SO_4 + 0.1 M NaOH (for pH 1.0–3.0), 0.2 M CH_3COOH + 0.2 M CH_3COONa (for pH 3.5–5.5), and 0.1 M NaH_2PO_4 + 0.1 M NaOH (for pH 6.0–13.0). Triply distilled water was deionized using TKA water purifier and used throughout the experiments. All other chem-

Published on the web October 4, 2005; DOI 10.1246/bcsj.78.1783

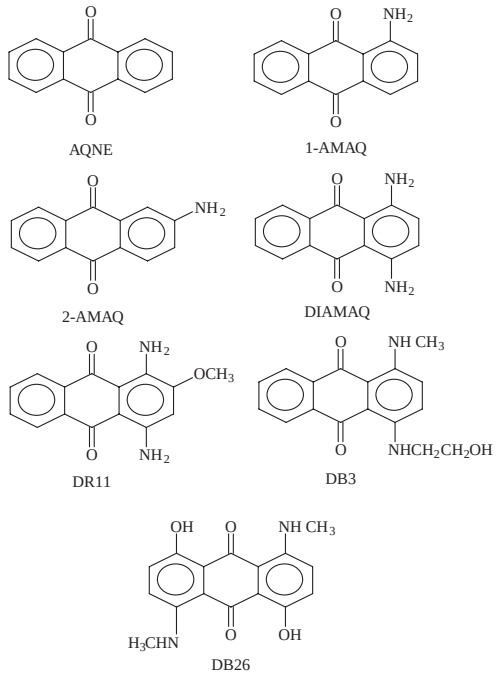

Scheme 1. Structures of the anthraquinone derivatives and dyes used.

icals used were of the highest purity available from Merck. Sodium montmorillonite clay was prepared by the ultrasonication of 1 g of montmorillonite SFG Clay (Acros Organics), 1 M sodium chloride and 20 mM CTAB for 4 h. After centrifugation, it was repeatedly washed with deionized triply distilled water, dialysed to remove the salt and dried.[28] 0.1 g of the resulted sodium montmorillonite clay (NaMM) in 10 mL triply distilled deionized water was stirred with 0.01% teflon for about 2 h to obtain 1% colloidal clay dispersion. N_2 and O_2 gases with purity 99.999% were used during the experiments.

Working Electrode Preparation. Two types of catalysts-incorporated sodium montmorillonite clay-modified glassy carbon electrodes were employed in the present investigation. One was catalyst adsorbed clay-modified GCE (GCE/NaMM/AQ). Clay films were produced by casting a known volume of 1% colloidal clay dispersion onto a clean and pretreated 0.0314 cm^2 GCE and drying under ambient conditions, usually from 0.5 to 1 h. GCE/NaMM/AQ was prepared by dropping a known volume of 0.001 M anthraquinone solutions over the clay film on clay-coated GCE and allowing the solvent to evaporate. The other working electrode was a catalyst–clay composite-modified GCE (GCE/NaMM–AQ composite), which was prepared by dropping a known volume of colloidal clay–catalyst composite dispersion, obtained by stirring 2 mL of clay colloid with 2 mL of 0.001 M anthraquinone solutions for 0.5 h and allowing the solvent to evaporate, on the surface of GCE. They were consequently rinsed with water and then transferred to an electrochemical cell for experiments. A three-electrode cell with a saturated calomel reference electrode (SCE), a platinum wire counter electrode, and an anthraquinone-incorporated clay-modified glassy carbon working electrode was employed. All electrochemical experiments were carried out at a thermostatic temperature of 25.0 ± 0.1 °C.

Apparatus. Cyclic voltammetry, chronoamperometry, and chronocoulometry were performed on an EG&G Princeton Applied Research Model 273A potentiostat/galvanostat (Princeton, NJ, USA) controlled by M270 software. A bi-potentiostat model AFRDE5 having an analytical rotator model AFMSRXE with MSRX speed control (PINE Instruments, USA) was employed for hydrodynamic voltammetric studies on dioxygen reduction.

Results and Discussion

Voltammetric studies of 9,10-anthraquinones-incorporated clay-modified electrodes were performed under deaerated and oxygen saturated conditions in the pH range 1.0–9.0, because of the unstable behavior of NaMM clay at a pH greater than 9.0.[30]

Electrochemical Behavior of 9,10-Anthraquinone-Incorporated CME. Cyclic voltammograms exhibited a single redox couple due to 9,10-anthraquinones in a deaerated solution at pH 1.0. Cyclic voltammetric responses of GCE/NaMM/2-AMAQ and GCE/NaMM–2-AMAQ composite in 0.1 mol dm^{-3} H_2SO_4 solution are presented in Figs. 1A and 1B, respectively. These voltammograms at various scan rates were studied to examine the variation of the peak current with the scan rates. The cathodic peak current increased linearly with square root of the scan rate $v^{1/2}$, indicating diffusion-controlled mass transfer. An increase in peak separation with an increase in scan rate proved the quasi-reversibility of the electron transfer process. A similar electrochemical behavior was observed for other anthraquinone derivatives and dyes.

Effect of pH: The voltammetric peak potentials are strongly pH dependent. The reduction peak potentials suffer cathodic shift towards more negative values, while increasing the pH of

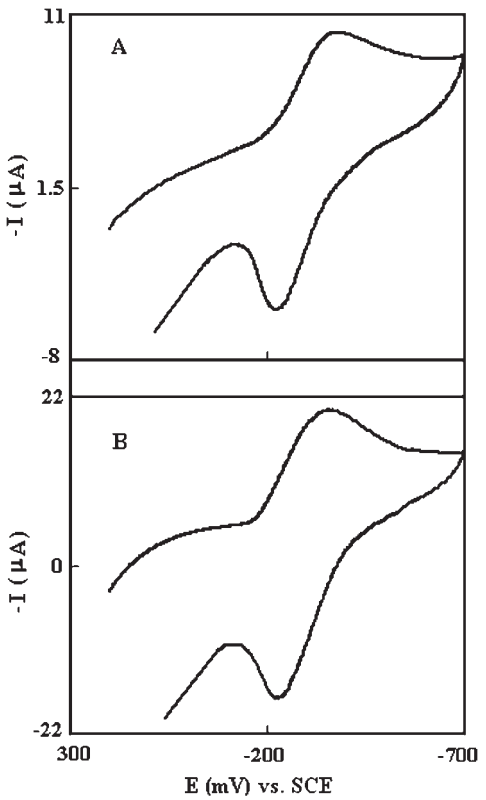

Fig. 1. Cyclic voltammograms in 0.1 mol dm^{-3} H_2SO_4 aqueous solution for A: GCE/NaMM/2-AMAQ and B: GCE/NaMM–2-AMAQ composite. Scan rate 40 mV s^{-1} Area of the electrode 0.0314 cm^2.

the solution. Since most of the anthraquinones-incorporated CMEs exhibited an irreversible cathodic peak at high pH, pH–cathodic peak potential diagrams were constructed. The E_{pc} vs pH plot consisted two distinct linear portions with different slopes of 59–62 mV at pH values of 1.0–8.0 and 27–30 mV at pH values above 8.0 per unit change in pH for AQNE, indicating the formation of three different forms of AQNE, one oxidized form (AQ) and its two reduced forms (AQH_2 and AQH^-) at the surface of both types of CMEs. Three distinct linear segments with different slopes of 87–91 mV at low pH values, 57–60 mV at intermediate pH values, and 28–31 mV at high pH values above 8.0 per unit change in pH were observed for the remaining six amino anthraquinone derivatives and dyes, indicating the existence of four different forms of amino anthraquinones, one oxidized form ($AQNH_2$) and its three reduced forms ($H_2AQNH_3^+$, H_2AQNH_2, and $HAQNH_2^-$) at the surface of both type CMEs. Figure 2 shows an illustrative cathodic peak potential vs pH plot for DR11 incorporated CMEs.

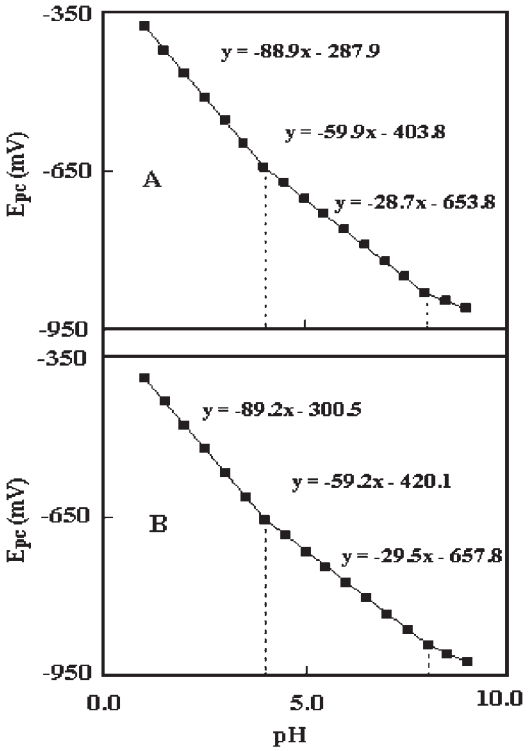

Fig. 2. pH–potential diagrams for A: GCE/NaMM/DR11 and B: GCE/NaMM–DR11 composite.

The electrode surface reaction at low pH values is a two-electron, three-proton process involving the formation of protonated hydroquinones;

$$AQNH_2 + 3H^+ + 2e^- \rightarrow H_2AQNH_3^+. \quad (1)$$

At low pH values, the protonation of the second amino group in DIAMAQ, DB3, DB26, and DR11 may be difficult due to the electron-withdrawing quarternary ammonium cation present in protonated anthraquinones.

In the intermediate pH range, the anthraquinone derivatives undergo a two-electron, two-proton process, producing the corresponding hydroquinones,

$$AQNH_2 + 2H^+ + 2e^- \rightarrow H_2AQNH_2. \quad (2)$$

At pH > 8.0, the electrode surface reaction is a two-electron one-proton process, which leads to the formation of a semihydroquinone anion,

$$AQNH_2 + H^+ + 2e^- \rightarrow HAQNH_2^-. \quad (3)$$

Effect of Substituents: The influence of 9,10-anthraquinone substituents on their electrochemical behavior was examined by comparing the cathodic peak potential in the neutral medium at which all anthraquinones used were reduced in a two-electron, two-proton process. As an illustration, the cathodic peak potentials of anthraquinones used at pH 7.0 are included in Table 1. It is interesting to note that electron donating substituents, structure, and symmetry of the molecule may cause a reduction at a high negative potential. The unsubstituted anthraquinone reduces at a lower potential than the amino substituted derivatives and dyes. 1-AMAQ reduces at a more negative potential (39.2 mV at catalyst adsorbed CME and 35.3 mV at catalyst–clay composite-modified GCE) as compared with 2-AMAQ, due to possible intramolecular H-bonding between the $-NH_2$ and –CO groups of 1-AMAQ, which may stabilize the anthraquininoid form. A similar observation was reported in earlier literature.[32] All of the remaining four catalysts reduced at high negative potentials near −800 mV, which may be due to the stronger hydrogen bonding between two amino groups and carbonyl groups. Anthraquinones re-

Table 1. Cathodic Peak Potential at pH 7.0 (E_{pc}), Diffusion Coefficients of 9,10-Anthraquinones (D) in NaMM Clay Films Obtained from Chronoamperometry, and Number of Electrons (n) Involved in the Reduction of Anthraquinones from Chronocoulometric Results

Anthraquinones	GCE/NaMM/AQ			GCE/NaMM–AQ composite		
	$-E_{pc}$ vs SCE /mV	$10^{10}D$ /cm^2 s^{-1}	n	$-E_{pc}$ vs SCE /mV	$10^{10}D$ /cm^2 s^{-1}	n
AQNE	616.3	6.94	1.99	630.7	8.23	2.00
1-AMAQ	767.8	0.85	2.01	782.5	1.69	2.02
2-AMAQ	728.6	1.37	2.06	747.2	2.54	1.98
DIAMAQ	815.4	3.59	2.03	813.5	4.49	1.99
DR11	824.5	5.24	2.01	835.2	3.58	1.99
DB3	817.8	5.08	2.01	839.6	2.23	1.98
DB26	795.4	5.17	2.00	806.1	2.82	2.01

duced at slight low negative potential on catalyst-adsorbed CME than on clay–catalyst composite-modified GCE. The reduction of anthraquinones on various modified electrodes at different potentials may be due to the existence of catalytic species in different orientations in the matrices of clay films.

Stability of the Anthraquinones-Incorporated CMEs. In order to examine the stability of the anthraquinones-incorporated CMEs and the reproducibility of their electrochemical behavior, thirty minutes of repetitive scanning between 0 and −700 mV at pH 1.0 and forty minutes of repetitive scanning between 0 to −1000 mV at pH 7.0 including more than 50 complete cyclic voltammograms under deaerated conditions were recorded. There were no measurable changes in the redox peak currents or separation of the peak. From the unaltered peak potentials and current observed in the cyclic voltammograms of 100 repetitive cycles at a scan rate of 40 mV/sec in oxygen saturated buffered solution of pH 7.0, the reproducibility of the electrocatalytic effect of the modified electrode was also ascertained.

Catalytic Reduction of Dioxygen at the Surface of CMEs. Electrocatalytic dioxygen reduction at 9,10-anthraquinones-incorporated CMEs was studied in different buffer media from pH 1.0 to 9.0. Although the reduction potentials of both dioxygen and anthraquinones are pH dependent,[20,24] their displacement may be unequal because of their different kinetic behavior. Thus, pH values of about 4.0–7.0 and 7.0–8.0 (depending on the nature of the modifying anthraquinone) were found to be the optimum pH (Tables 2 and 3) for anthraquinones adsorbed CMEs and anthraquinones–clay composite-modified GCEs, respectively, where the cathodic peak reached its maximum current and the maximum dioxygen reduction potential shift (ΔE) was observed. This shift (ΔE) is the difference between the oxygen reduction potential at anthraquinone-incorporated clay-modified electrodes and that at bare GCE. For instance, Figure 3 exhibits a variation of the dioxygen reduction potential shift with the pH for GCE/NaMM/AQNE and GCE/NaMM–AQNE composite. Here, the maximum shift was observed at pH 7.0. Hu[30] studied this reduction using a sodium montmorillonite–methyl viologen carbon paste chemically modified electrode at pH 7.0. It was also reported that dioxygen is reduced bioelectrocatalytically to water at neutral pH.[5,33]

Cyclic voltammograms of CMEs incorporated with anthraquinones in the absence and presence of oxygen were compared with the corresponding voltammograms at bare GCE. As an example, dioxygen reduces at bare GCE irreversibly with a peak potential of −1020.9 mV in the phosphate buffer pH 7.0. 1-AMAQ shows a larger enhancement in the cathodic peak current of CMEs (Fig. 4) under an O_2 saturated condition with the disappearance of the anodic peak, suggesting the electrocatalytic reduction of dioxygen. The reduction of oxygen occurred at −786.2 and −825.1 mV on GCE/NaMM/1-AMAQ and GCE/NaMM–1-AMAQ composite, respectively. Thus, the modified CMEs incorporated with 1-AMAQ caused a shift in the oxygen reduction potential by about 234.7 and 195.8 mV for 1-AMAQ adsorbed on clay and 1-AMAQ–clay composite, respectively. The observed shifts with the different anthraquinones investigated at their optimum pH are presented in Tables 2 and 3. As is obvious from the data, the dispersed dyes caused lesser a shift in the dioxygen reduction potential

Table 2. Optimum pH (pH), Dioxygen Reduction Potential Shift (ΔE), Surface Coverage (N_p), Number of Electrons Involved (n), Mass Specific Current (M.S.C.), Heterogeneous Rate Constant (k), and Diffusion Coefficient (D_{O_2}) of O_2 in the Electrocatalytic Reduction of O_2 at the Surface of Anthraquinones Adsorbed Clay-Modified Electrodes

Anthraquinones	pH	ΔE /mV	$10^{10}N_p$ /mol cm^{-2}	n	M.S.C. /A mg^{-1}	$10^{-4}k$ /M^{-1} s^{-1}	$10^5 D_{O_2}$ /cm^2 s^{-1}
AQNE	7	452.1	3.28	3.96	20.77	1.44	1.42
1-AMAQ	7	234.7	11.94	4.01	8.95	1.13	1.41
2-AMAQ	5	173.8	9.70	4.05	10.08	1.15	1.36
DIAMAQ	7	193.0	9.25	3.98	9.74	1.13	1.39
DR11	7	242.5	4.62	3.99	11.72	1.09	1.31
DB3	7	236.7	6.42	4.03	9.46	1.09	1.45
DB26	4	228.0	4.62	4.08	10.40	1.02	1.48

Table 3. Optimum pH (pH), Dioxygen Reduction Potential Shift (ΔE), Surface Coverage (N_p), Number of Electrons Involved (n), Mass Specific Current (M.S.C.), Heterogeneous Rate Constant (k), and Diffusion Coefficient (D_{O_2}) of O_2 in the Electrocatalytic Reduction of O_2 at the Surface of Anthraquinones-Composite Clay-Modified Electrodes

Anthraquinones	pH	ΔE /mV	$10^{10}N_p$ /mol cm^{-2}	n	M.S.C. /A mg^{-1}	$10^{-4}k$ /M^{-1} s^{-1}	$10^5 D_{O_2}$ /cm^2 s^{-1}
AQNE	7	421.0	1.67	4.01	27.51	1.58	1.46
1-AMAQ	7	195.8	4.94	4.07	14.18	1.11	1.43
2-AMAQ	7	230.0	4.27	3.99	15.55	1.19	1.40
DIAMAQ	8	180.4	3.22	4.02	14.73	1.03	1.48
DR11	7	190.0	6.74	4.06	10.47	1.19	1.37
DB3	7	150.0	4.64	3.97	10.90	1.09	1.46
DB26	7	128.2	4.35	3.98	10.49	1.01	1.42

in dyes–clay composite-modified GCE than in dyes adsorbed clay-modified GCE. Under O_2 saturated conditions, the cathodic peak current, I_{pc}, is linearly proportional to square root of the scan rate, $v^{1/2}$, indicating diffusion-limited reduction.[3,25]

Chronoamperometric Studies. A double potential-step technique at initial and final potentials of 0.0 and −800 mV vs SCE was employed to examine the chronoamperometric behavior of plain and 9,10-anthraquinones-incorporated clay-modified GC electrodes in the absence and presence of O_2. For instance, chronoamperograms of plain GCE and 2-AMAQ adsorbed clay-modified GCE in the presence and absence of O_2 at pH 5.0 are illustrated in Figs. 5A and 5B, respectively. The net electrolysis current (I_{net}) was determined by point-to-point subtraction of the background current in the presence and absence of O_2. Under deaerated conditions, a plot of net current against $t^{-1/2}$ shows a straight line (Fig. 5C line d), which extrapolates close to the origin. Since the oxidized and reduced forms of the anthraquinone derivatives are known to be insoluble in water, such a near Cottrellian behavior may be explained by finite diffusion in thin films.[3,20,21,24] From the slope of I vs $t^{-1/2}$ plots under deaerated conditions, the diffusion coefficient values of anthraquinones used in the two types of CMEs were determined using the Cottrell equation;

$$I = nFD^{1/2}AC_p\pi^{-1/2}t^{-1/2}, \quad (4)$$

$$\text{Slope} = nFD^{1/2}AC_p\pi^{-1/2}. \quad (5)$$

Here, C_p (mol cm^{-3}) is the concentration of the electroactive anthraquinone in the clay film, D (cm^2 s^{-1}) is the diffusion coefficient of the anthraquinone in clay films, and A (cm^2) is the geometric area of the GC electrode. The concentration of the electroactive species, C_p,[34] was determined using the relation $C_p = N_p/Al$, where N_p is the amount of electroactive species on the surface of the clay-modified electrode and l is the film thickness. The surface coverage of the electroactive species, N_p, was determined from cyclic voltammograms at low scan rates (5 mV s^{-1}) using the relation $N_p = Q/nFA$, where Q is the charge consumed, n the number of electrons involved in the reduction of catalyst, and F (96485 C mol^{-1}) the Faraday constant. The calculated D values are given in Table 1 and N_p values are summarized in Tables 2 and 3. It is noteworthy that, the N_p values of anthraquinone and its amino derivatives in catalyst-adsorbed CMEs are greater than in catalyst-composite-modified electrodes. This is most probably indicative of the greater occupation of intercalation sites by catalysts and the presence of less disordered zones in composite-modified

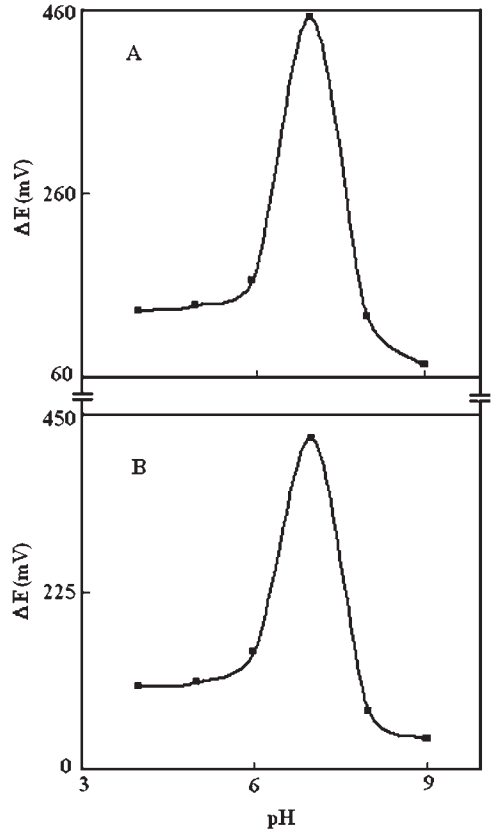

Fig. 3. Plots of pH vs shift in O_2 reduction potential at A: GCE/NaMM/AQNE and B: GCE/NaMM–AQNE composite.

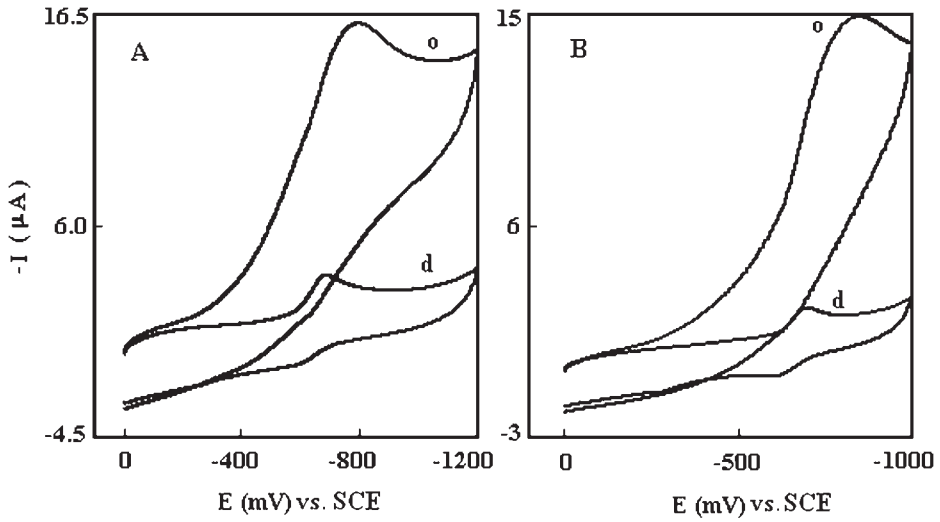

Fig. 4. Cyclic voltammograms of A: GCE/NaMM/1-AMAQ and B: GCE/NaMM–1-AMAQ composite in the absence (d) and presence (o) of dioxygen at pH 7.0. Area of the electrode 0.0314 cm^2.

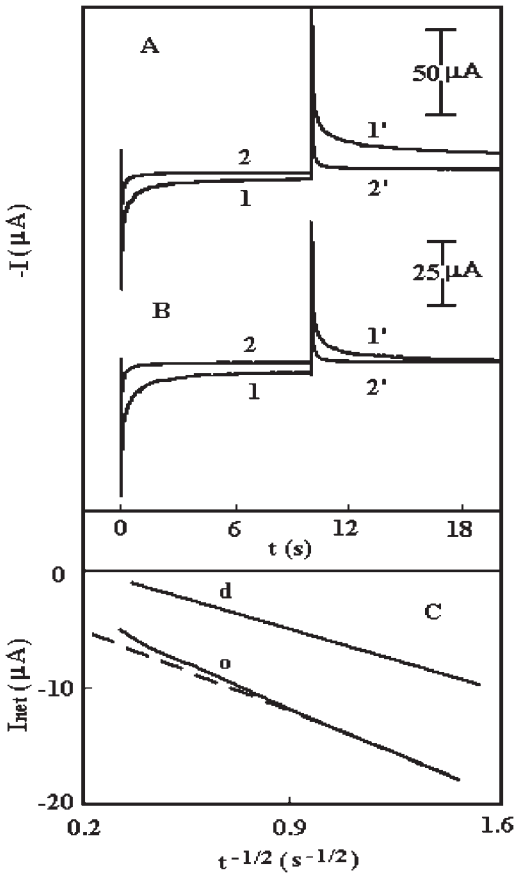

Fig. 5. Chronoamperograms obtained in pH 5.0 by the double potential-step technique at an initial potential of 0.0 mV and final potential of −800 mV vs SCE. A: 1,1′ for GCE/NaMM/2-AMAQ in the O_2-saturated buffer. 2,2′ as 1,1′ for the plain GCE. B: 1,1′ for GCE/NaMM/2-AMAQ under deaerated condition, 2,2′ as 1,1′ for the plain GCE. C: Plots of net current vs $t^{-1/2}$ for the above clay-modified GCE in the absence (d) and presence (o) of dioxygen.

electrodes. It is already reported that with more defects, the probability that clay-bound catalysts have access to the electrode surface is increased.[10,11] The diffusion coefficient values of anthraquinone and its amino derivatives in catalyst-composite modified electrodes are slightly greater than in catalyst adsorbed CMEs. On the other hand, the dispersed dyes have slightly lower diffusion coefficient values in composite-modified electrodes than in catalyst-adsorbed CMEs. Depending upon the pore size of the clay, the structure and symmetry of the molecules, catalysts diffuse with different rates through the clay films.

In dioxygen saturated buffer, the corresponding Cottrell plot, I_{net} vs $t^{-1/2}$ (Fig. 5C line o), is linear at short time periods, while it deviates from linearity at longer times. The extrapolation of the linear part of the plot I_{net} vs $t^{-1/2}$ results in an intercept at about 5.08 μA. This transient current is largely due to the catalytic reduction of dioxygen by the 2-AMAQ used, since the direct reduction of O_2 at a plain electrode shows only little residual current. A similar behavior was also observed for other anthraquinone derivatives and dyes.

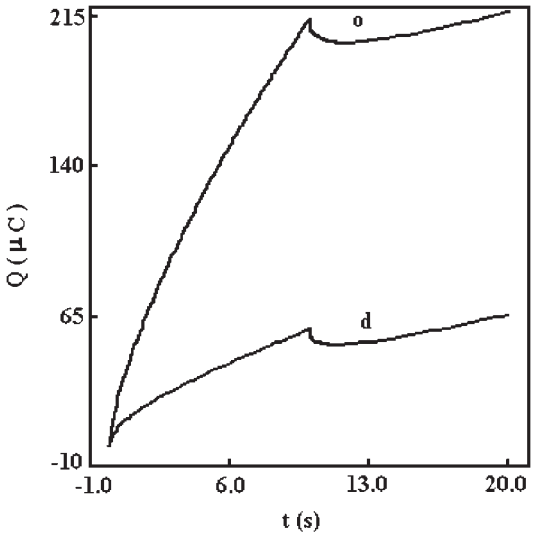

Fig. 6. Chronocoulometric curves of GCE/NaMM–AQNE composite at pH 7.0 in the absence (d) and presence (o) of dioxygen.

Chronocoulometric Studies. Chronocoulometric behavior of plain GCE and anthraquinones-incorporated CMEs was investigated in the absence and presence of oxygen by performing a double potential-step technique with initial and final potentials of 0.0 and −800 mV vs SCE. For instance, the chronocoulogram for a 9,10-anthraquinone–clay composite-modified electrode under deaerated and oxygen saturated conditions at pH 7.0 is presented in Fig. 6. In oxygenated buffer, there is a large enhancement in charge, indicating the electrocatalytic reduction of dioxygen. The same behavior was observed for the other anthraquinone derivatives and dyes. From the slope of Q vs $t^{1/2}$ plots under deaerated conditions, the number of electrons (n) involved in the reduction of anthraquinones at the optimum pH was calculated by employing the diffusion coefficient values of anthraquinones obtained from the chronoamperometric results. The calculated n values are closer to 2.0, and are included in the Table 1. The number of the electrons (n) involved in dioxygen reduction at anthraquinones-incorporated CMEs was also determined from the slope of Q vs $t^{1/2}$ plots under oxygen saturated conditions using the Cottrell equation,

$$Q = 2nFACD^{1/2}\pi^{-1/2}t^{1/2}, \quad (6)$$

where $C = 1.25$ mM, $A = 0.0314$ cm^2, and $D = 1.57 \times 10^{-5}$ cm^2 s^{-1}, as presented in Tables 2 and 3. The total number of electrons involved in the reduction of oxygen is found to be 4.0, and hence the reduction product is water.[30]

Hydrodynamic Voltammetric Studies on Dioxygen Reduction. For a more quantitative assessment of the kinetic parameters, the electrocatalytic reduction of O_2 was examined at rotating clay-modified electrodes incorporated with anthraquinone derivatives and dyes used at their optimum pH. Figure 7A shows a set of current–potential curves recorded in an O_2 saturated buffer of pH 7.0 at various angular velocities, ω, with a rotating DB3 adsorbed clay-modified GC electrode. Curve a is the response of the modified electrode in the absence of O_2. The small limiting current observed here may

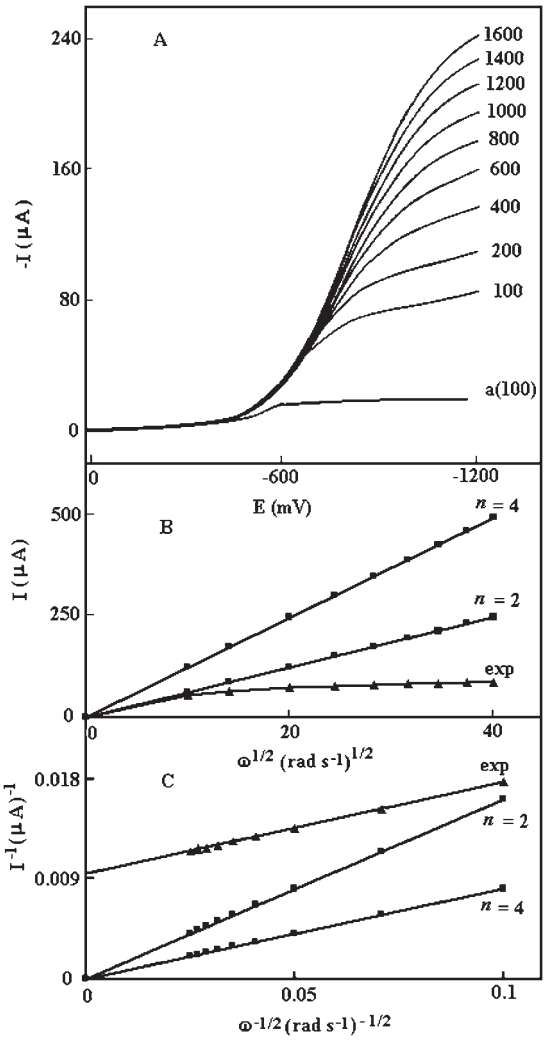

Fig. 7. A: Current–potential curves at different rotation rates (rpm), B: Levich plots, and C: Koutecky–Levich plots for the reduction of dioxygen at a rotating DB3 adsorbed clay-modified electrode in the buffered solution of pH 7.0.

have been due to reduction of the catalyst. The limiting current, I_l, is defined as the difference between the currents on a modified electrode at the potential corresponding to the diffusion plateau in deaerated and O_2-saturated solutions.[3,20,21,25] At $\omega = 100$ rpm, the mass specific activity of anthraquinones in dioxygen reduction was determined,[35] and is included in Tables 2 and 3. The Levich plot, derived from the limiting current measured at a potential of −950 mV (Fig. 7B), is non-linear, as expected for a catalytic reduction in which a current-limiting chemical step precedes the electron transfer. Similar results are also reported in earlier literature.[3,20,21,24] As shown in Fig. 7C, the corresponding Koutecky–Levich plot is linear, with a slope close to that of the theoretical line for the reduction of O_2 via four electrons, which indicates the accomplishment of the reduction of O_2 to H_2O by the anthraquinones-incorporated clay-modified electrodes. The unit-cell formula for montmorillonite in the sodium form[30] is $[(Si_{7.84}Al_{0.16})(Fe^{3+}{}_{0.26}Al_{3.22}Mg_{0.40}Fe^{2+}{}_{0.12})O_{20}(OH)_4Na_{0.68}]$. Diffusion of the adsorbed electroactive species through the film, electron hopping between the adsorbed species and the iron cation present in the clay films contribute to the electron transport in CMEs.[34] According to earlier reports,[27,28,30] some mediators incorporated clay film is an efficient catalyst for the reduction of hydrogen peroxide to water; this electrochemical activity relies mainly on the iron cation in the clay. Based on the above discussion, the mechanism for dioxygen reduction, which involves two catalytic steps, has been proposed as follows:

$$2AQ + 4e^- + 2H^+ \rightarrow AQH_2 + AQ^{2-}. \quad (7)$$

First, the catalytic step:

$$AQH_2 + O_2 \rightarrow AQ + H_2O_2. \quad (8)$$

Second, the catalytic step:

$$AQ^{2-} + 2Fe^{3+} \rightarrow AQ + 2Fe^{2+}, \quad (9)$$

$$2Fe^{2+} + H_2O_2 + 2H^+ \rightarrow 2Fe^{3+} + 2H_2O. \quad (10)$$

Thus, mediators shuttle electrons between the electrodes and substrate molecules in electrochemical catalysis, thereby facilitating the dioxygen reduction to water. Zhang and Anson[36] also reported the involvement of four electrons in dioxygen reduction. A similar behavior was observed in the case of other 9,10-anthraquinone derivatives and dyes.

The rate constant for the catalytic reaction between the reduced anthraquinone AQH_2 and O_2 is obtained from the Koutecky–Levich plots using the following expression:

$$I_l{}^{-1} = I_k{}^{-1} + I_{lev}{}^{-1} = [nFAkC_{O_2}N_p]^{-1} + [0.62nFAD_{O_2}{}^{2/3}v^{-1/6}\omega^{1/2}C_{O_2}]^{-1}, \quad (11)$$

where C_{O_2} is the bulk concentration of O_2, ω is the rotational speed, v is the hydrodynamic viscosity, N_p is the amount of anthraquinone on the surface of the clay-modified GC electrode, k is the rate constant, and all the remaining parameters have their usual meanings. From the intercepts of the Koutecky–Levich plots, the rate constants for the dioxygen reduction were evaluated, and are summarized in Tables 2 and 3. The diffusion coefficient of O_2 at rotating CMEs incorporated with anthraquinones in oxygen saturated aqueous buffer was determined using the Levich equation, and is reported in Tables 2 and 3, which are comparable with the reported values.[24,25] The values of kinematic viscosity of water v, and the concentration of O_2 in solution C_{O_2} used in this calculation were 0.01 $cm^2\ s^{-1}$ and 1.25 mM,[3,20] respectively.

Conclusion

This work describes the preparation of anthraquinones adsorbed clay-modified GC electrodes and anthraquinones-composite modified GC electrodes and their electrocatalytic behavior towards dioxygen reduction. The cathodic peak potential of the anthraquinones was shifted toward a more negative direction with increasing pH of the supporting media. The diffusion coefficient values of anthraquinone and its amino derivatives are slightly greater in catalyst-composite modified electrodes than in adsorbed clay-modified electrodes, but dispersed dyes have lower diffusion coefficient values in composite-modified electrodes as compared to in adsorbed CMEs. Hydrodynamic voltammetric and chronocoulometric studies showed the in-

volvement of four electrons in the dioxygen reduction at 9,10-anthraquinones-incorporated clay-modified electrodes. The heterogeneous rate constants for the reduction of O_2 at the surface of these modified electrodes are greater than the data reported for 1,4-dihydroxy anthraquinones-modified glassy carbon electrodes.[24] These clay-modified electrodes offer the possibility for developing a sensitive method to detect the presence of dissolved oxygen.

References

1 E. L. Dewi, K. Oyaizu, H. Nishide, and E. Tsuchida, *J. Power Sources*, **130**, 286 (2004).

2 A. Ayad, Y. Naimi, J. Bouet, and J. F. Fauvarque, *J. Power Sources*, **130**, 50 (2004).

3 A. Salimi and M. Ghadermazi, *Anal. Sci.*, **17**, 1165 (2001).

4 "Fuel Cell Handbook," 5th ed, ed by M. C. Williams, Department of Energy, Washington, US (2000).

5 S. Tsujimura, M. Kawaharada, T. Nakagawa, K. Kano, and T. Ikeda, *Electrochem. Commun.*, **5**, 138 (2003).

6 M. E. Lai and A. Bergel, *J. Electroanal. Chem.*, **494**, 30 (2000).

7 H. Naohara, S. Ye, and K. Uosaki, *Electrochim. Acta*, **45**, 3305 (2000).

8 V. Ganesan and R. Ramaraj, *J. Appl. Electrochem.*, **30**, 757 (2000).

9 Z. Navratilova and P. Kula, *Electroanalysis*, **15**, 837 (2003).

10 G. Villemure and A. J. Bard, *J. Electroanal. Chem.*, **282**, 107 (1990).

11 P. Joo, *Colloids Surf.*, **49**, 29 (1990).

12 M. B. Vukmirovic, N. Vasiljevic, N. Dimitrov, and K. Sieradzki, *J. Electrochem. Soc.*, **150**, B10 (2003).

13 L. Mao, D. Zhang, T. Sotomura, K. Nakatsu, N. Koshiba, and T. Ohsaka, *Electrochim. Acta*, **48**, 1015 (2003).

14 R. Gonzalez-Cruz and O. Solorza-Feria, *J. Solid State Electrochem.*, **7**, 289 (2003).

15 R. Chithra and R. Renuka, *J. Appl. Electrochem.*, **33**, 443 (2003).

16 Y. Zhang, S. Asahina, S. Yoshihara, and T. Shirakashi, *Electrochim. Acta*, **48**, 741 (2003).

17 G. Ramirez, E. Trollund, M. Isaacs, F. Armijo, J. Zagal, J. Costamagna, and M. J. Aguirre, *Electroanalysis*, **14**, 540 (2002).

18 A. S. Lin and J. C. Huang, *J. Electroanal. Chem.*, **541**, 147 (2003).

19 S. Peressini, C. Tavagnacco, G. Costa, and C. Amatore, *J. Electroanal. Chem.*, **532**, 295 (2002).

20 P. Manisankar, A. M. Pushpalatha, S. Vasanthkumar, A. Gomathi, and S. Viswanathan, *J. Electroanal. Chem.*, **571**, 43 (2004).

21 S. Golabi and J. B. Raoof, *J. Electroanal. Chem.*, **416**, 75 (1996).

22 A. Sarapuu, K. Vaik, D. J. Schiffrin, and K. Tammeveski, *J. Electroanal. Chem.*, **541**, 23 (2003).

23 K. Tammeveski, K. Kontturi, R. J. Nichols, R. J. Potter, and D. J. Schiffrin, *J. Electroanal. Chem.*, **515**, 101 (2001).

24 A. Salimi, M. F. Mousavi, H. Sharghi, and M. Shamsipur, *Bull. Chem. Soc. Jpn.*, **72**, 2121 (1999).

25 A. Salimi, H. Eshghi, H. Sharghi, S. M. Golabi, and M. Shamsipur, *Electroanalysis*, **11**, 114 (1999).

26 P. V. Kamat, *J. Electroanal. Chem.*, **163**, 389 (1984).

27 N. Oyama and F. C. Anson, *J. Electroanal. Chem.*, **199**, 467 (1986).

28 J. M. Zen, S. H. Jeng, and H. J. Chen, *J. Electroanal. Chem.*, **408**, 157 (1996).

29 N. Oyama, N. Oki, H. Ohno, Y. Ohnuk, H. Matsuda, and E. Tsuchida, *J. Phys. Chem.*, **87**, 3642 (1983).

30 S. Hu, *J. Electroanal. Chem.*, **463**, 253 (1999).

31 S. Fukuzumi, K. Okamoto, Y. Tokuda, C. P. Gros, and R. Guilard, *J. Am. Chem. Soc.*, **126**, 17059 (2004).

32 M. Shamsipur, A. Salimi, S. M. Golabi, H. Sharghi, and M. F. Mousavi, *J. Solid State Electrochem.*, **5**, 68 (2001).

33 S. Tsujimura, H. Tatsumi, J. Ogawa, S. Shimizu, K. Kano, and T. Ikeda, *J. Electroanal. Chem.*, **496**, 69 (2001).

34 A. Ramasubbu, A. Vanangamudi, S. Muthusubramanian, M. S. Ramachandran, and S. Sivasubramanian, *Electrochem. Commun.*, **2**, 56 (2000).

35 S. R. Brankovic, J. X. Wang, and R. R. Adzic, *Electrochem. Solid-State Lett.*, **4**, A217 (2001).

36 J. Zhang and F. C. Anson, *J. Electroanal. Chem.*, **353**, 265 (1993).